Physics and Experiments
with Future Linear e+e- Colliders
Sitges

D. Dominici

Phenomenology of the lightest Pseudo Nambu Goldstone boson at future colliders

- **R. Casalbuoni**
- **A. Deandrea**
- **S. De Curtis**
- **R. Gatto**
- **J. F. Gunion**

http://alphateo.fi.infn.it/~dominici/talks/sitges.ps

The framework

- A strong breaking of the electroweak symmetry (technicolor with extended technicolor, walking technicolor, ...)

- A low energy effective theory with a chiral symmetry group $G \to H$ (breaking induced, for instance, by a technifermion condensate $< \bar{T}T >$).

- Example. One-family model $T \equiv (U, D, N, E)$.

  $$G = SU(8)_L \times SU(8)_R \qquad H = SU(8)_{L+R}$$

  Goldstones belong to G/H. These are massless until the $G_W = SU(3) \times SU(2) \times U(1)$ interactions are introduced.

- The masses of the vector resonances will be of the order of TeV

- The masses of colored PNGB's are in general quite large

- We focus on the lightest PNGB (P^0)

  $$20\ GeV \leq m_{P^0} \leq 200\ GeV$$

- The DSB model will be specified by a low energy effective Lagrangian

Table of PNGB

The 63 Goldstone bosons with their quantum numbers and transformation properties under $SU(2)_L$ and $SU(3)_c$ (here $Y = 2(Q - T^3)$ is the hypercharge):

	$SU(2)_L$	$SU(3)_c$	Q	Y
π^+ $(\tilde{\pi}^+)$ π^- $(\tilde{\pi}^-)$ π^3 $(\tilde{\pi}^3)$	3	1	1 -1 0	0
π_D	1	1	0	0
π_8^α	1	8	0	0
$\pi_8^{\alpha+}$ $\pi_8^{\alpha-}$ $\pi_8^{\alpha 3}$	3	8	1 -1 0	0
P_3^{0i} $(\bar{P}_3^{0i})$	1	3	$\frac{2}{3}$ $(-\frac{2}{3})$	$\frac{4}{3}$ $(-\frac{4}{3})$
P_3^{+i} $(\bar{P}_3^{+i})$ P_3^{-i} $(\bar{P}_3^{-i})$ P_3^{3i} $(\bar{P}_3^{3i})$	3	3	$\frac{5}{3}$ $(-\frac{5}{3})$ $-\frac{1}{3}$ $(\frac{1}{3})$ $\frac{2}{3}$ $(-\frac{2}{3})$	

The effective Lagrangian

- Gauge Lagrangian

The low energy effective lagrangian will contain interaction terms among the PNGB's and the ordinary gauge bosons, collected in $\mathcal{L}_g$ (Chada and Peskin):

$$\mathcal{L}_g = \frac{v^2}{16} Tr\left(\mathcal{D}_\mu U^\dagger \mathcal{D}_\mu U\right)$$

where

$$U = \exp\left(\frac{2iT^s\pi^s}{v}\right)$$

with $v = 246\ GeV$. T^s $(s = 1, \ldots, 63)$ are the $SU(8)$ generators.
The covariant derivative $\mathcal{D}_\mu U$ is given by

$$\mathcal{D}_\mu U = \partial_\mu U + \mathcal{A}_\mu U - U\mathcal{B}_\mu$$

where

$$\mathcal{A}_\mu = igT^a W_\mu^a + ig'\frac{T_D}{\sqrt{3}}B_\mu + i\frac{g_s}{\sqrt{2}}T_8^\alpha G_\mu^\alpha$$

$$\mathcal{B}_\mu = ig'T^3 B_\mu + ig'\frac{T_D}{\sqrt{3}}B_\mu + i\frac{g_s}{\sqrt{2}}T_8^\alpha G_\mu^\alpha$$

W_μ^a $(a = 1, 2, 3)$, B_μ and G_μ^α $(\alpha = 1, \cdots, 8)$, are the gauge vector fields related to the gauge group G_W.

- Yukawa Lagrangian (Casalbuoni et al)

In order to write the Yukawa couplings between the Goldstone bosons and the ordinary fermions we decompose the matrix U according to

$$U = \begin{pmatrix} U^{ij}_{uu} & U^{ij}_{ud} & U^{k}_{u\nu} & U^{k}_{ue} \\ U^{ij}_{du} & U^{ij}_{dd} & U^{k}_{d\nu} & U^{k}_{de} \\ U^{l}_{\nu u} & U^{l}_{\nu d} & U_{\nu\nu} & U_{\nu e} \\ U^{l}_{eu} & U^{l}_{ed} & U_{e\nu} & U_{ee} \end{pmatrix} \qquad i,j,k = 1,2,3$$

The most general Yukawa coupling invariant with respect to G_W is given by

$$\begin{aligned}
\mathcal{L}_Y = \; & - \; m_1 \left(\bar{t}^i_R U^{\dagger ij}_{uu} t^j_L + \bar{t}^i_R U^{\dagger ij}_{du} b^j_L \right) - m_2 \left(\bar{b}^i_R U^{\dagger ij}_{ud} t^j_L + \bar{b}^i_R U^{\dagger ij}_{dd} b^j_L \right) \\
& - \; m_4 \left(\bar{\tau}_R U^{\dagger}_{\nu e} \nu_{\tau L} + \bar{\tau}_R U^{\dagger}_{ee} \tau_L \right) - m^{(2)}_4 \left(\bar{\mu}_R U^{\dagger}_{\nu e} \nu_{\mu L} + \bar{\mu}_R U^{\dagger}_{ee} \mu_L \right) \\
& - \; m_5 \left(\bar{t}^i_R U^{\dagger jj}_{uu} t^i_L + \bar{t}^i_R U^{\dagger jj}_{du} b^i_L \right) - m_6 \left(\bar{b}^i_R U^{\dagger jj}_{ud} t^i_L + \bar{b}^i_R U^{\dagger jj}_{dd} b^i_L \right) \\
& - \; m_7 \left(\bar{t}^i_R U^{\dagger}_{\nu\nu} t^i_L + \bar{t}^i_R U^{\dagger}_{e\nu} b^i_L \right) - m_9 \left(\bar{b}^i_R U^{\dagger}_{\nu e} t^i_L + \bar{b}^i_R U^{\dagger}_{ee} b^i_L \right) \\
& - \; m_{10} \left(\bar{\tau}_R U^{\dagger jj}_{ud} \nu_{\tau L} + \bar{\tau}_R U^{\dagger jj}_{dd} \tau_L \right) \\
& - \; m^{(2)}_{10} \left(\bar{\mu}_R U^{\dagger jj}_{ud} \nu_{\mu L} + \bar{\mu}_R U^{\dagger jj}_{dd} \mu_L \right) \\
& - \; m_{11} \left[\bar{t}_R \lambda^\alpha \begin{pmatrix} U^{\dagger}_{uu} & U^{\dagger}_{du} \end{pmatrix} \begin{pmatrix} \lambda^\alpha & 0 \\ 0 & \lambda^\alpha \end{pmatrix} \begin{pmatrix} t_L \\ b_L \end{pmatrix} \right] \\
& - \; m_{12} \left[\bar{b}_R \lambda^\alpha \begin{pmatrix} U^{\dagger}_{ud} & U^{\dagger}_{dd} \end{pmatrix} \begin{pmatrix} \lambda^\alpha & 0 \\ 0 & \lambda^\alpha \end{pmatrix} \begin{pmatrix} t_L \\ b_L \end{pmatrix} \right] \\
& + \; \cdots + h.c.
\end{aligned}$$

As usual, the magnitudes of the Yukawa couplings are most naturally set by the scale of the corresponding fermionic masses.

- In the (U, D, N, E) realization of our model, the U_{uu}, U_{dd}, $U_{\nu\nu}$ and U_{ee} entries above come from techni-U, D, N and E fermion propagator loop corrections, respectively.

- In a multiscale technicolor model, the above would be generalized by writing $\mathcal{L}_g$ and $\mathcal{L}_Y$ as a sum of terms with different v_i $(v_i \leq v)$.

Expanding to first order in $1/v$, we have

$$\begin{aligned}
U_{uu}^{ij} &\sim \delta^{ij}\left[1 + \frac{i}{v}\sqrt{6}\frac{P^{0\prime}}{3}\right] + \ldots \\
U_{dd}^{ij} &\sim \delta^{ij}\left[1 - \frac{i}{v}\sqrt{6}\frac{P^{0}}{3}\right] + \ldots \\
U_{\nu\nu} &\sim \left[1 - \frac{i}{v}\sqrt{6}P^{0\prime}\right] + \ldots \\
U_{ee} &\sim \left[1 + \frac{i}{v}\sqrt{6}P^{0}\right] + \ldots
\end{aligned}$$

with

$$P^0 = \frac{\tilde{\pi}_3 - \pi_D}{\sqrt{2}}, \qquad P^{0\prime} = \frac{\tilde{\pi}_3 + \pi_D}{\sqrt{2}}$$

or

$$P^0 = \frac{1}{\sqrt{12}}(3E\overline{E} - D\overline{D}) \quad P^{0\prime} = \frac{1}{\sqrt{12}}(U\overline{U} - 3N\overline{N})$$

which are purely $T_3 = -1/2$ and $T_3 = +1/2$ weak isospin states.

From the $\mathcal{O}(1)$ terms in the expansion of $\mathcal{L}_Y$ we easily recover the expressions for the fermion masses

$$m_t = m_1' + m_7 \quad m_b = m_2' + m_9$$

$$m_\tau = m_4 + 3m_{10} \quad m_\mu = m_4^{(2)} + 3m_{10}^{(2)}$$

$$m_{\nu_\tau} = m_{\nu_\mu} = 0$$

where

$$m_1' \equiv m_1 + 3m_5 + \frac{16}{3}m_{11} \qquad m_2' \equiv m_2 + 3m_6 + \frac{16}{3}m_{12}$$

Evaluate one-loop effective potential

$$m_{P^0}^2 = \frac{4\Lambda^2}{\pi^2 v^2}(2m_2'm_9 + 2m_4m_{10} + 2m_4^{(2)}m_{10}^{(2)})$$

$$m_{P^{0\prime}}^2 = \frac{4\Lambda^2}{\pi^2 v^2}2m_1'm_7$$

Λ is the UV cut-off, situated in the TeV region.

Note no $P^0 - P^{0\prime}$ mixing and $m_{P^\pm}^2 = \frac{1}{2}(m_{P^0}^2 + m_{P^{0\prime}}^2)$.

- A very crucial point: P^0 and $P^{0\prime}$ are the mass eigenstates

m_{P^0} comes from terms involving b, τ, μ

$$\Rightarrow m_{P^0} << m_{P^{0\prime}}$$

- P^0 couplings, widths

The P^0 boson couples to the $T_3 = -1/2$ component of the fermion doublets (while $P^{0\prime}$ couples to the $T_3 = +1/2$ component):

$$\mathcal{L}_Y = -i\lambda_b \bar{b}\gamma_5 b P^0 - i\lambda_\tau \bar{\tau}\gamma_5 \tau P^0 - i\lambda_\mu \bar{\mu}\gamma_5 \mu P^0$$

with

$$\lambda_b = -\frac{\sqrt{6}}{3v}\left(m_2' - 3m_9\right) \quad \lambda_\tau = \frac{\sqrt{6}}{v}\left(m_4 - m_{10}\right)$$

$$\lambda_\mu = \frac{\sqrt{6}}{v}\left(m_4^{(2)} - m_{10}^{(2)}\right)$$

The P^0 boson couples to gauge bosons via ABJ anomaly:

$$g_{PV_1V_2} = \alpha N_{TC}\frac{A_{PV_1V_2}}{\pi v}\epsilon_{\lambda\mu\nu\rho}p_1^\lambda \epsilon_1^\mu p_2^\nu \epsilon_2^\rho$$

where for $P = P^0$ we have:

$$\begin{aligned}
A_{P^0\gamma\gamma} &= -\frac{4}{\sqrt{6}}\left(\frac{4}{3}\right) \\
A_{P^0Z\gamma} &= -\frac{4}{2\sqrt{6}}\left(\frac{1-4s_W^2}{4s_W c_W} - \frac{t_W}{3}\right) \\
A_{P^0ZZ} &= -\frac{4}{\sqrt{6}}\left(\frac{1-2s_W^2}{2c_W^2} - \frac{t_W^2}{3}\right) \\
A_{P^0gg} &= \frac{1}{\sqrt{6}}
\end{aligned}$$

where $s_W = \sin\theta_W$, *etc.*.

A special choice for this study

$$m'_1 = m_7 = \frac{m_t}{2} \quad m'_2 = m_9 = \frac{m_b}{2}$$

$$m_{10} = -m_4 = \frac{m_\tau}{2} \quad m^{(2)}_{10} = -m^{(2)}_4 = \frac{m_\mu}{2}$$

The corresponding one-loop P^0 and $P^{0\prime}$ masses are

$$m^2_{P^0} = \frac{2\Lambda^2}{\pi^2 v^2} m_b^2 \quad m^2_{P^{0\prime}} = \frac{2\Lambda^2}{\pi^2 v^2} m_t^2$$

$$\Rightarrow m_{P^0} \sim 8 \text{ GeV} \times \Lambda(\text{TeV})$$

The corresponding fermionic couplings

$$\lambda_b = \sqrt{\frac{2}{3}} \frac{m_b}{v}, \quad \lambda_\tau = -\sqrt{6} \frac{m_\tau}{v}, \quad \lambda_\mu = -\sqrt{6} \frac{m_\mu}{v}$$

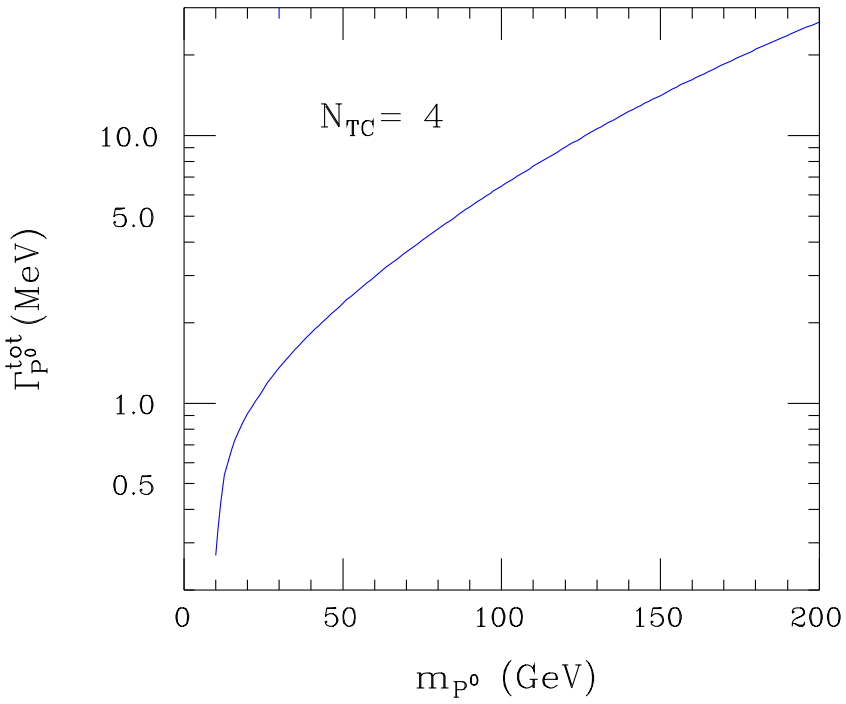

Branching ratios for P^0 decay

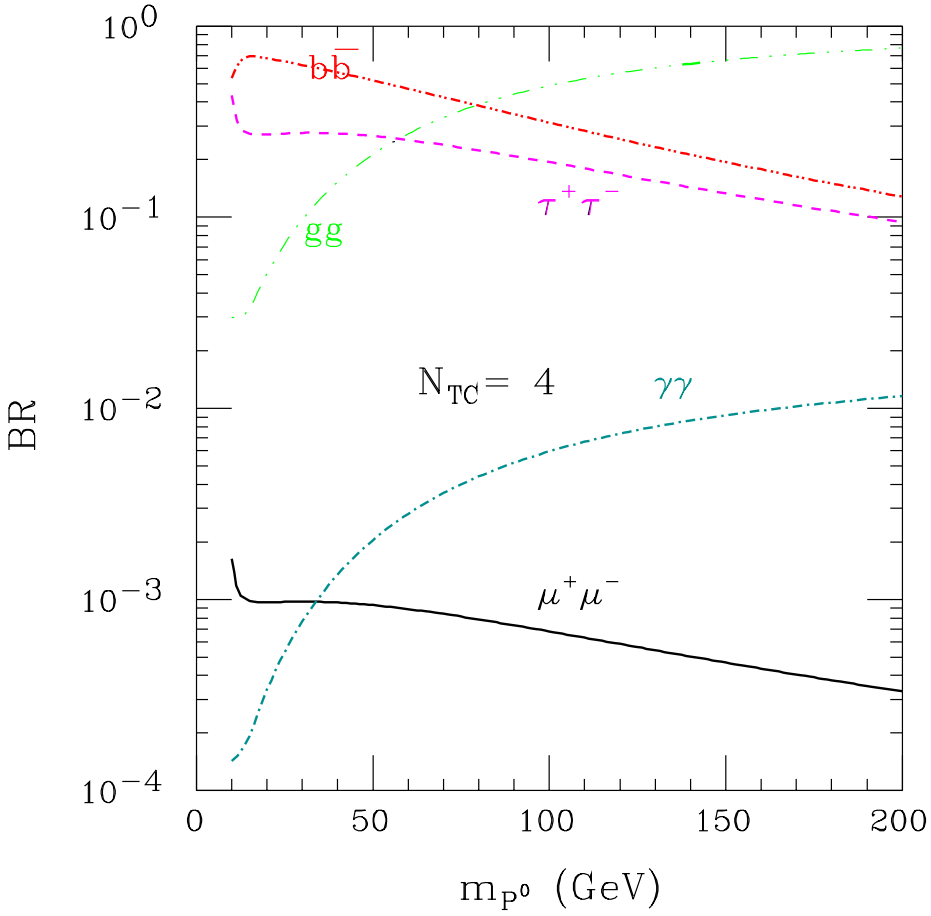

- Notice

$$\frac{,(P^0 \to gg)B(P^0 \to \gamma\gamma)}{,(h \to gg)B(h \to \gamma\gamma)} \sim 10^2 \quad 50 \lesssim m_{P^0/h}(GeV) \lesssim 150$$

(h is the SM Higgs boson). This makes P^0 discovery possible at LHC in the

$$gg \to P^0 \to \gamma\gamma$$

channel for

$$30 - 50 \lesssim m_{P^0}(GeV) \lesssim 150 - 200$$

or perhaps also at RunII Tevatron ($S/\sqrt{B} \geq 3$ for $m_{P^0} \gtrsim 60$).

Ratios of branching ratios

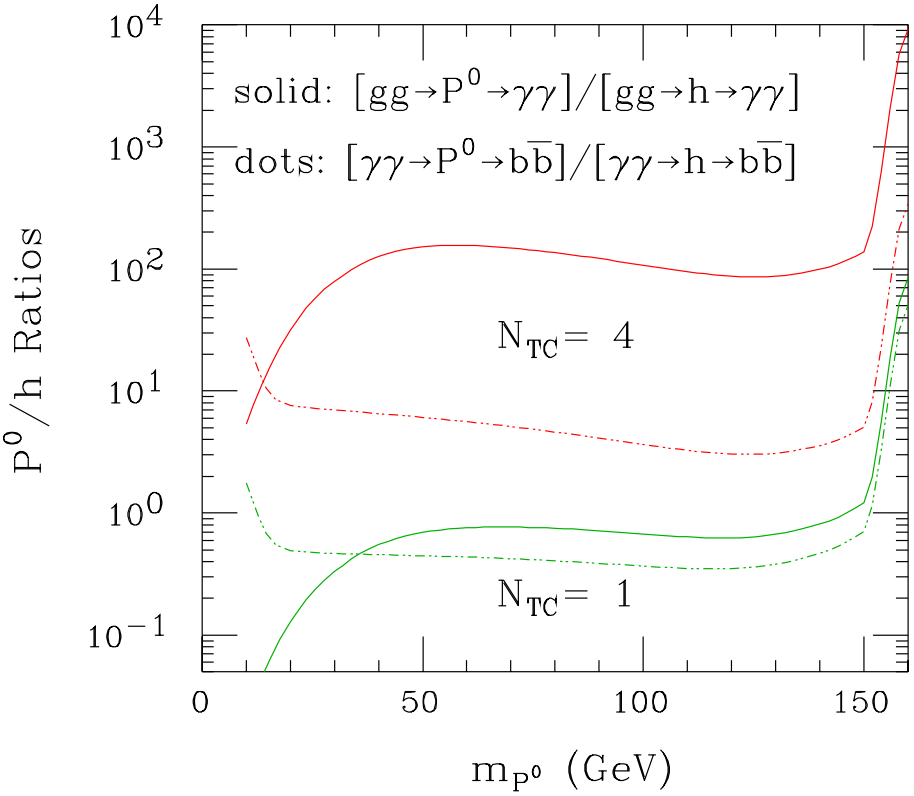

- The ratios

  $[,(P^0 \to gg)B(P^0 \to \gamma\gamma)]/[,(h \to gg)B(h \to \gamma\gamma)]$

  (solid curves) and

  $[,(P^0 \to \gamma\gamma)B(P^0 \to b\bar{b})]/[,(h \to \gamma\gamma)B(h \to b\bar{b})]$

  (dotted curves)
  are plotted as a function of m_{P^0}, taking $m_h = m_{P^0}$.
  Results are given for $N_{TC} = 4$ and $N_{TC} = 1$.

Limits on P^0 from LEP

- At LEP the dominant production mode is $Z \to \gamma P^0$ (Manohar and Randall)

$$, (Z \to \gamma P^0) = \frac{\alpha^2 m_Z^3}{96\pi^3 v^2} N_{TC}^2 A_{P^0 Z\gamma}^2 \left(1 - \frac{m_{P^0}^2}{m_Z^2}\right)^3$$

Let us require that the $Z \to \gamma P^0$ decay width be $> 2 \times 10^{-6}$ GeV in order for the P^0 to be visible in a sample of 10^7 Z bosons. The minimum N_{TC} value required as a function of m_{P^0} is plotted in figure. We see that $N_{TC} \gtrsim 8$ is required at $m_{P^0} = 0$, rising rapidly as m_{P^0} increases.

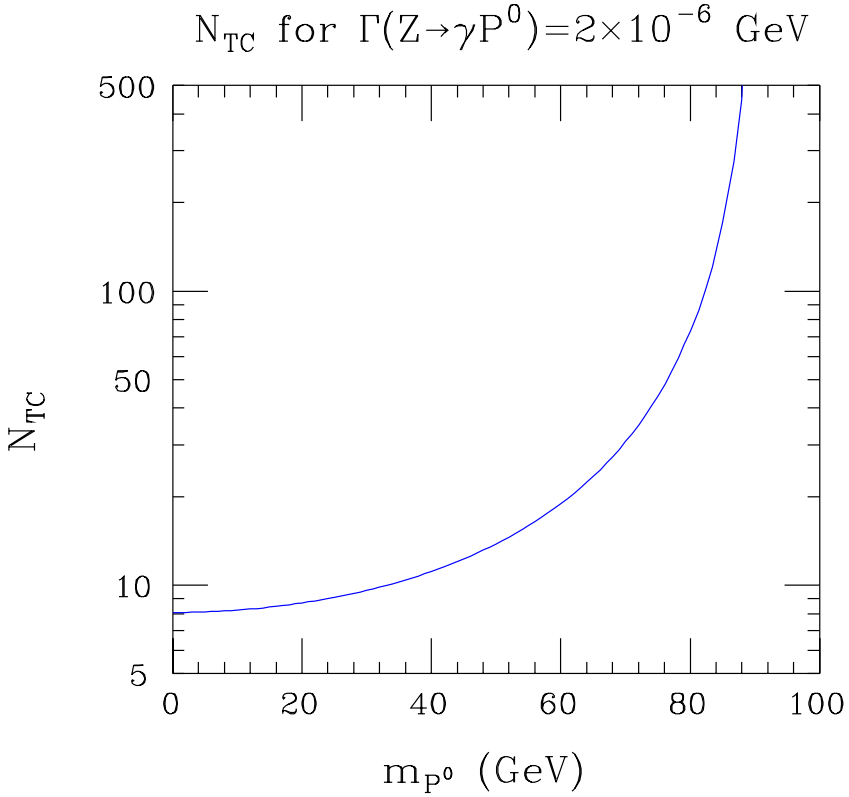

Results at future e^+e^-

- The dominant production mode is $e^+e^- \to \gamma P^0$ via γ and Z exchange.

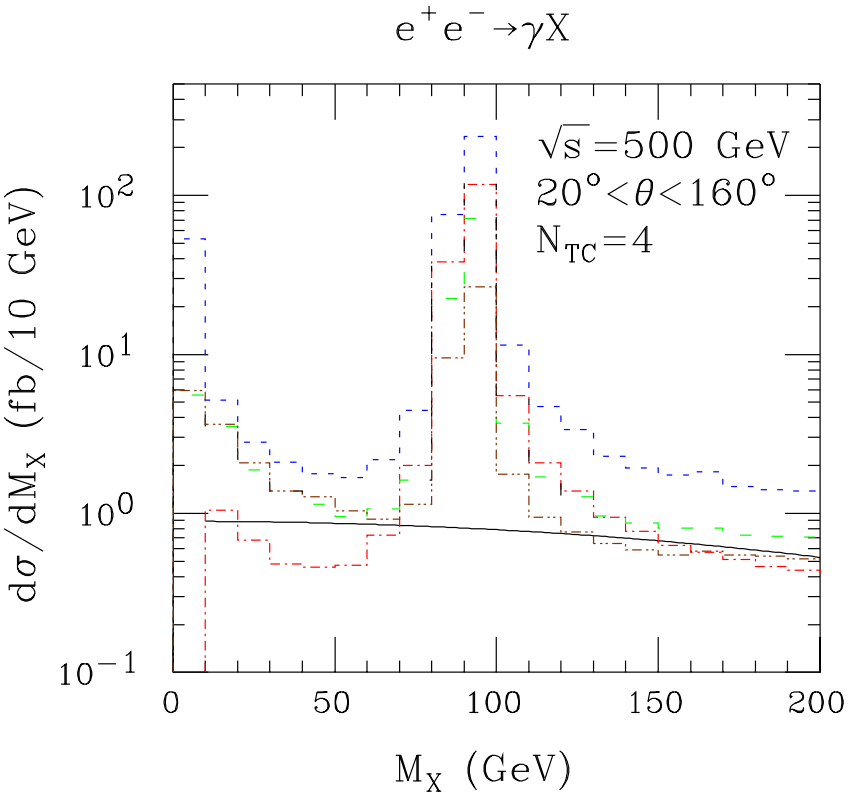

- The cross section (in fb) for $e^+e^- \to \gamma P^0$ (solid curve) is plotted as a function of m_{P^0} in comparison to various possible backgrounds: $e^+e^- \to \gamma b\bar{b}$ (dotdash); $e^+e^- \to \gamma c\bar{c}$ (dashes); $e^+e^- \to \gamma q\bar{q}$, $q = u, d, s$ (small dashes); and $e^+e^- \to \gamma\tau^+\tau^-$ (dashdoubledots). The background cross sections are integrated over a $\Delta M_X = 10$ GeV bin. A cut of $20^\circ \leq \theta \leq 160^\circ$ has been applied to avoid photon collinear singularity. Effects due to tagging and mistagging are also included.

For $L = 500$ fb^{-1} we have from 2500 to 4500 P^0 evts.

- Statistical significance in various tagged channels in $e^+e^- \to \gamma P^0$

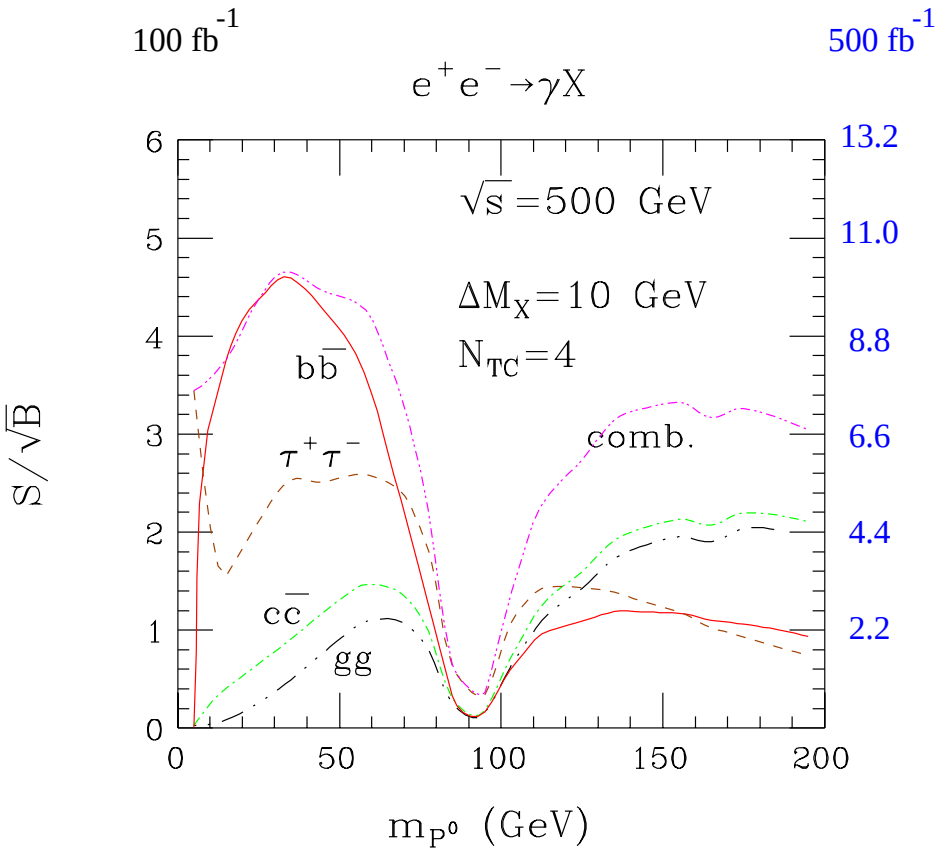

For $L = 100$ fb^{-1}

$$\frac{S}{\sqrt{B}} \geq 3 \qquad m_P^0 \leq 75 \text{ GeV}, \quad m_P^0 \geq 130 \text{ GeV}$$

For TESLA 500 fb^{-1}, $\frac{S}{\sqrt{B}}$ multiplied by a factor ~ 2.2.

- After discovery, one can determine branching fractions in various channels and couplings. The only channel with reasonable ($\lesssim 15\%$) statistical error would be $b\bar{b}$, for $L = 500$ fb^{-1}.

- Statistical errors for various tagged channels in $e^+e^- \to \gamma P^0$

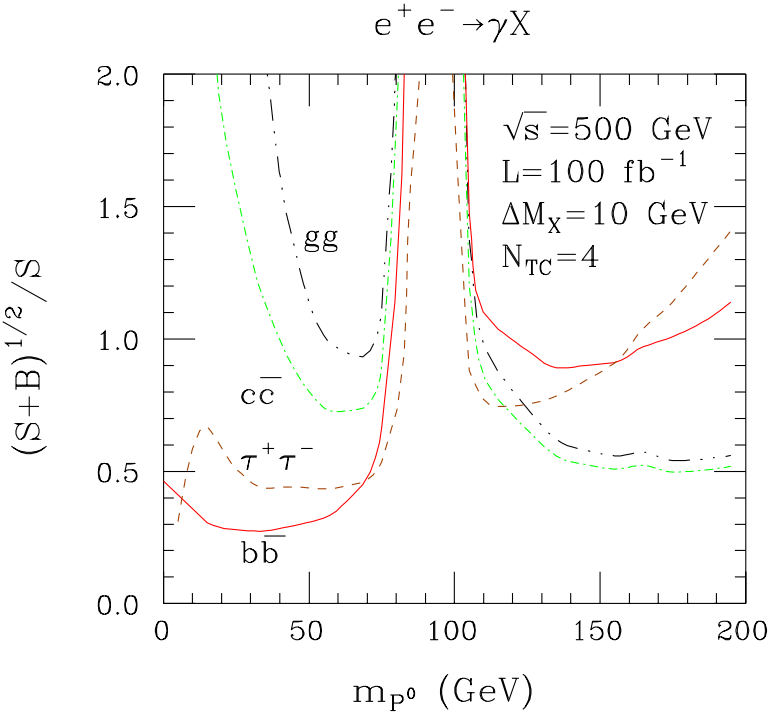

- The next step is the model-independent determination of

$$B(P^0 \to X) = \frac{\sigma(e^+e^- \to \gamma P^0) B(P^0 \to X)}{\sigma(e^+e^- \to \gamma P^0)}$$

The crucial issue is then the ability to observe the P^0 inclusively in the γX final state as a peak in the recoil M_X spectrum, and the associated error in the inclusive cross section $\sigma(e^+e^- \to \gamma P^0)$. The resolution in M_X is determined by the photon energy resolution. $\Delta E_\gamma/E_\gamma = 0.12/\sqrt{E_\gamma} \oplus 0.01 \Rightarrow \pm 1\sigma$ mass windows in m_{P^0} of [0, 78], [83.5, 114] and [193, 207] (GeV units) for $m_{P^0} = 55$, 100 and 200 GeV, respectively. Difficult, especially for low m_{P^0}.

Results at future $\gamma\gamma$

By folding the cross section for the P^0 production at a given energy $E_{\gamma\gamma}$ of a $\gamma\gamma$ collider with the differential luminosity

$$N(\gamma\gamma \to P^0 \to X) = \frac{8\pi,\ (P^0 \to \gamma\gamma)B(P^0 \to X)}{m^2_{P^0} E_{e^+e^-}} \tan^{-1} \frac{,\ \text{exp}}{,\ \text{tot}_{P^0}} \times \left(1 + \langle\lambda\lambda'\rangle\right) G(y_0) L_{e^+e^-}$$

where $y_0 = m_{P^0}/E_{e^+e^-}$, λ and λ' are the helicities of the colliding photons, , exp is the mass interval accepted in the final state. For initial discovery one chooses initial laser circular polarizations and e^+e^- helicities for a broad spectrum ($2\lambda_e P_c = +1$). One has $G(y_0) \gtrsim 1$ and $\langle\lambda\lambda'\rangle \sim 0.8$.

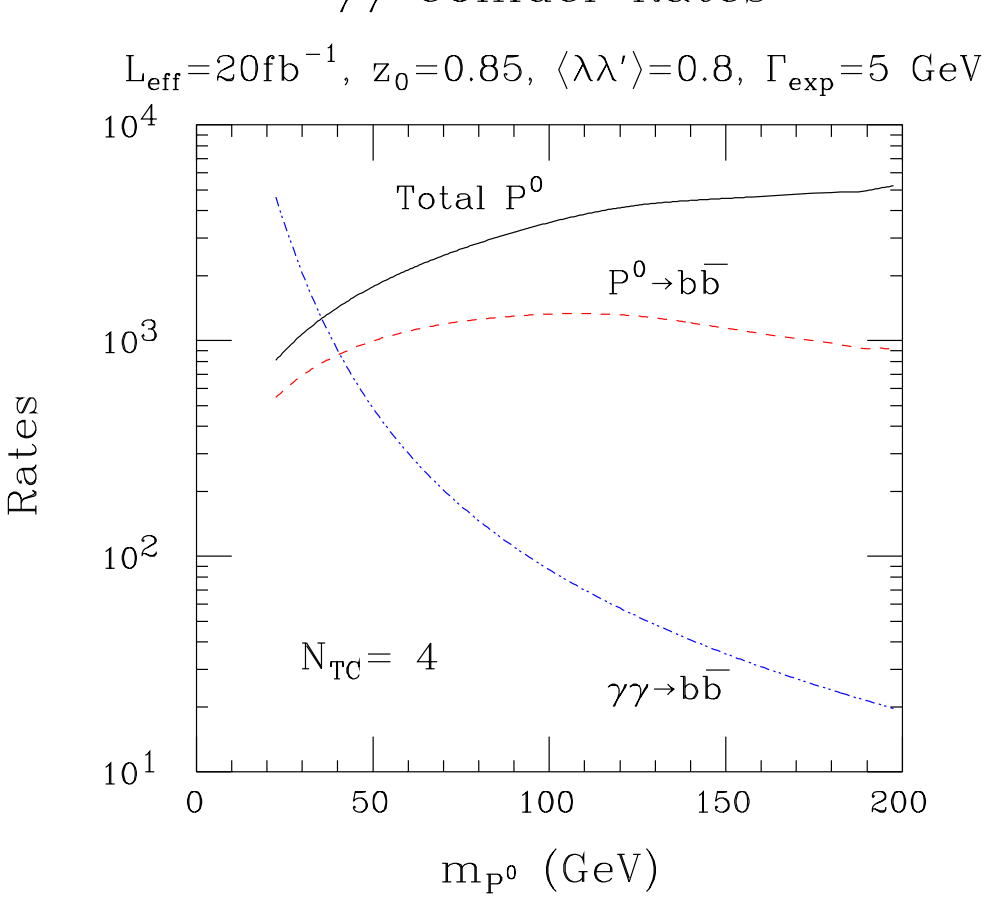

Angular cut $|\cos\theta| \leq z_0$. $L_{eff} \equiv G(y_0) L_{e^+e^-}$.

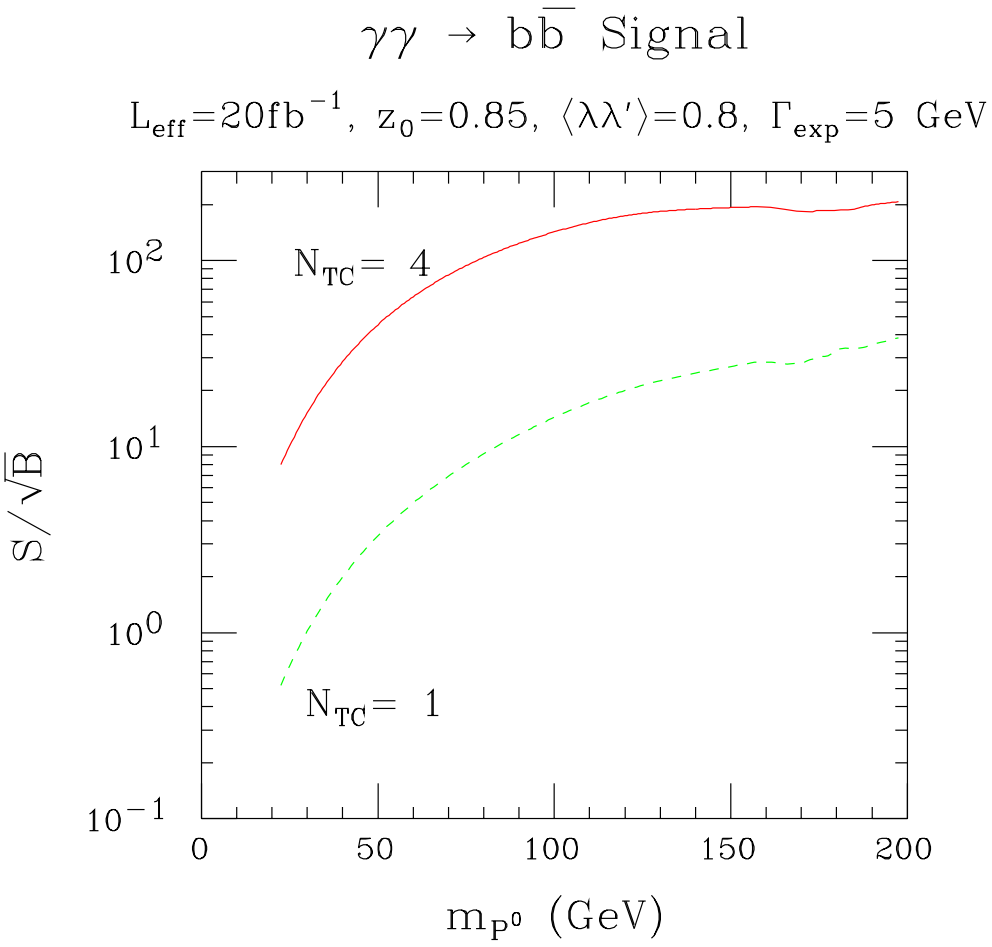

- Once the P^0 has been discovered, one can configure the $\gamma\gamma$ collision set-up so that the luminosity is peaked at $E_{\gamma\gamma} \sim m_{P^0}$. A very precise measurement of the P^0 rate in the $b\bar{b}$ final state will then be possible if $N_{TC} = 4$.
  Assuming $L = 10$ fb^{-1}, for the 106 GeV $\leq m_{jj} \leq$ 126 GeV mass window, a statistical error for measuring , $(P^0 \rightarrow \gamma\gamma)B(P^0 \rightarrow b\bar{b})$ of $\lesssim 1.5\%$. Systematic errors will probably dominate.

s – channel P^0 production at $\mu^+\mu^-$

- The P^0 has a sizeable $\mu^+\mu^-$ coupling
- The muon collider has the ability to achieve a very narrow Gaussian spread, $\sigma_{\sqrt{s}} \sim 1$ MeV $\left(\frac{R}{0.003\%}\right)\left(\frac{\sqrt{s}}{50\ \text{GeV}}\right)$ One can achieve $R = 0.003\%$ beam energy resolution with reasonable luminosity (L_{year}(@100 GeV) = 0.1 fb^{-1}).
- Good measurements of rates $\mu^+\mu^- \to b\bar{b}, \tau^+\tau^-, gg$ and , $^{\text{tot}}_{P^0}$.

In conclusion

- , $^{\text{tot}}_{P^0}$ from the muon collider
- , $(P^0 \to gg)B(P^0 \to \gamma\gamma)$ from the LHC
- , $(P^0 \to \gamma\gamma)B(P^0 \to b\bar{b})$ from the $\gamma\gamma$
- , $(P^0 \to \mu^+\mu^-)B(P^0 \to F)$ for $F = b\bar{b}, \tau^+\tau^-, gg$ from the muon collider

determine the number of technicolors of the theory and (up to a discrete set of ambiguities) the fundamental parameters of the low-energy effective Lagrangian describing the Yukawa couplings of the P^0.

Conclusions

- Loose limits on P^0 from existing measurements
- Discovery at Run II Tevatron is possible for $N_{TC} = 4$ and $m_P^0 \geq 60$ GeV at 3-4σ level
- LHC could discover the P^0 in the $50 - 200$ GeV range with a precise measurement of , $(P^0 \to gg)B(P^0 \to \gamma\gamma)$
- Discovery could be possible also at an e^+e^- collider for $L = 100$ (500) fb^{-1} and $\sqrt{s} = 500$ GeV at 3σ level for $m_{P^0} \leq 75$ (80) GeV and $m_{P^0} \geq 135$ (105) GeV. $\gamma\gamma$ option more robust and allows a precise measurement of , $(P^0 \to \gamma\gamma)B(P^0 \to b\bar{b})$
- If P^0 discovered at LHC or/and e^+e^-, a $\mu^+\mu^-$ collider can scan and center on $\sqrt{s} = m_{P^0}$ within $\sigma_{\sqrt{s}}$, making an accurate determination of its mass. Four years of running at $\sqrt{s} = m_{P^0} \Rightarrow b\bar{b}, gg, \tau^+\tau^-$ rates and , $^{\text{tot}}_{P^0}$ to $\leq 10\%$